

Analysis of broadened Mössbauer spectra using simple mathematical functions

Analysis of broadened Mössbauer spectra

A. Cabral-Prieto

© Springer Science+Business Media Dordrecht 2013

Abstract Simulated and experimental broadened Mössbauer spectra are analyzed using several distribution functions. The resolution Hesse and Rübartsch data are reproduced in order to analyze the origin of the oscillations appearing in the recovered distribution function. The lined triangular distribution is used and some of its properties are described. The no implicit n th-nomial distribution function $P(x) = (a\cos(\pi x) + b\sin(\pi x))^n$ is introduced, complementing the Window and Hesse and Rübartsch no implicit distribution functions. This new no implicit distribution function gives similar results of those of Window's method. In addition, the Window method has also been modified by inserting a smoothing factor λ_C . For $0 < \lambda_C < 1$ a hyperfine distribution with low resolution may be obtained; for $\lambda_C > 1$, the opposite is obtained. The Levenberg-Marquardt algorithm is used to solve the involved Fredholm integral equation rather than the typical second order regularized algorithm. From the extracted hyperfine field distribution functions of the Mössbauer spectra of the amorphous and crystallized $\text{Fe}_{70}\text{Cr}_2\text{Si}_5\text{B}_{16}$ magnetic alloy the short range atomic order for the amorphous state of this alloy can be inferred.

Keywords Mössbauer spectroscopy · No implicit and implicit hyperfine distributions · Amorphous alloys · Short range atomic order

1 Introduction

Broad Mössbauer spectra are frequently obtained from materials where slightly different iron sites are present; examples such as amorphous magnetic alloys [1–10];

Proceedings of the Thirteenth Latin American Conference on the Applications of the Mössbauer Effect, (LACAME 2012), Medellín, Colombia, 11–16 November 2012.

A. Cabral-Prieto (✉)
Depto. de Química, Instituto Nacional de Investigaciones Nucleares,
Apdo. Postal 18-1027, Col. Escandón,
Deleg. M. Hidalgo, C. P. 11801, México D. F., México
e-mail: agustin.cabral@inin.gob.mx

nanometric materials with crystal size distribution(s), like goethite [8], hidrotalcites containing iron, stainless steels, etc. [1–10]. The hyperfine parameters of the Mössbauer spectra of these materials (isomer shift δ , quadrupole splitting Δ , and the hyperfine magnetic field H) are usually evaluated as distribution functions ($P(x)$ with $x = \delta$, or Δ , or H) rather than as discrete values. Several methods have appeared in the literature where a sum of magnetic patterns (1) or an implicit distribution like the Gaussian line are used [1, 7, 8, 11]. Others methods assume no implicit expressions for the $P(x)$ distribution. Whereas Window [2] describes $P(x)$ in terms of a Fourier series expansion (FSE), Hesse and Rübartsch [3] use a discrete step function. According to this line of thought, the n th nomial distribution function $P(x) = (a\cos(\pi x) + b\sin(\pi x))^n$ assumes neither a previous knowledge of the $P(x)$ distribution, and is introduced in this study. The resulting distributions from this new function are practically similar to those obtained from the Window method [3]. The implicit lined triangle distribution function is also introduced in this study. In addition to these new proposed no-implicit and implicit distribution functions the Window method has been modified by inserting a smoothing factor λ_C which can take the values $0 > \lambda_C \geq 1$. For a highly resolved distribution function a $\lambda_C > 1$ is required. This smoothing factor multiplies the trigonometric argument of the Cosine or Sine function appearing in the Window method [2].

Generally speaking, one can get practically the same results using anyone of these three no-implicit distributions functions (Window, Hesse and Rübartsch, and present methods). Particularly, the Hesse and Rübartsch method is faster than the others but it is basically limited to one parameter, the number of points of the distribution (NSUB), to get a well resolved distribution. The Window method originally had the number of terms of the FSE in order to obtain a well resolved distribution. The introduction of the smoothing factor λ_C in the present work gives an additional parameter in order to optimize a solution. Similarly the new n th-nomial distribution function depends on the number of terms ($n + 1$) of the distribution. In addition to this, the later no implicit distribution handles even and odd functions simultaneously. This property would allow studying them in a future work in order to see if it is possible to reduce the oscillations that appear in any solution of these no implicit methods.

2 Experimental

The resolution Hesse and Rübartsch data consisting of a magnetic sextet modified by two Gaussian distribution functions centered at 17.5 and 20 T of standard deviation $\sigma = 0.85$ T each are reproduced [3]. The above simulated spectrum and those of the amorphous and crystallized soft magnetic $\text{Fe}_{77}\text{Cr}_2\text{Si}_5\text{B}_{16}$ alloy (S3A alloy from Metglas) are analyzed by using the unmodified and modified Window methods [2] and the new proposed distribution function.

3 Methodology

Present analysis assumes the thin absorber approximation where the resonance line is a Lorentzian distribution of FWHM $\Gamma = 0.194$ mm/s. In the transmission

Mössbauer set up, a broadened magnetic Mössbauer spectrum can be represented by the Fredholm integral of the first kind as

$$S_{calc} = \int_c^d P(B) L_6(v, B) dB, \tag{1}$$

where $S_{calc}(v)$ is the calculated spectrum as a function of the relative velocity between the absorber and Mössbauer source. $L_6(v, B)$ stands for the magnetic sextet of normalized Lorentzian lines and $P(B)$ is the unknown probability distribution function of the hyperfine magnetic field B . The condition $\int_c^d P(B)dB = 1$ has to be met if quantitative information is required from the measured spectrum $S_m(v)$.

The solution of integral equation (1) needs a careful numerical treatment because the resulting hyperfine distribution(s) and the fitted spectrum may posses an oscillatory behavior due to statistical fluctuations on the experimental data set $S_m(v)$ or rounding errors (3, 7, 9). In order to solve this problem several regularized algorithms are at hand. Singular Value Decomposition (SVD), Truncated Singular Value Decomposition (TSVD), Generalized SVD (GSVD), the Tikhonov-Arsenine regularization or the Philips-Twomey regularization methods are some of them. The Tikhonov regularization methods are classified as zero, first and second order regularization algorithms. Any of these algorithms regularizes the ill-posed problem derived from the solution of integral equation (1). From the author’s perspective, the preferred algorithm used in Mössbauer spectroscopy is the Philips-Twomey or Tikhonov second order regularization method after proposing it by Hesse and Rübartsch [3]. The zero and first order regularization algorithms, or the SVD, TSVD GSVD have been little explored. The Levenberg-Marquadt (LM) algorithm, which is the standard routine to solve non-linear problems, may also be considered as the Tikhonov zero order regularization method, and is used in the present work. The resulting normal equations of this algorithm may be written as

$$(J^T J + \lambda_{LM} I) \Delta x = J^T b, \tag{2}$$

where J represents the Jacobian matrix and J^T its transpose, λ_{LM} is the Levenberg-Marquardt factor that controls the searching route to obtain the “best solution” between the Gauss-Newton and the Steepest-Descent methods, I is the identity matrix; λ_{LM} is an internal parameter of the computing program and one has not to worry about it; b represents the weighted residuals between the measured data $S_m(v)$ and the calculated $S_{calc}(v)$ ones. Expression (2) is practically the same as that of the standard form of Tikhonov zero order regularization algorithm

$$(J^T J + \lambda_T I) \Delta x_T = J^T b \tag{3}$$

The goal of the Tikhonov λ_T factor in (2) is to provide a “smooth solution” of the desired hyperfine $P(x)$ distribution and of the fitted spectrum $S_c(v)$. In this case, the Tikhonov λ_T factor is user defined. Technically, the effect of both the LM and Tikhonov factors, λ_{LM}, λ_T in (2) and (3), respectively, is to dampen the contributions of small singular values in the solution of the $J^T J$ matrix.

Thus the Levenberg-Marquadt algorithm can, under certain conditions, be considered the same to the Tikhonov zero order regularization. Thus, a first introspection of the solutions that can provide the LM algorithm is presented using several distribution functions.

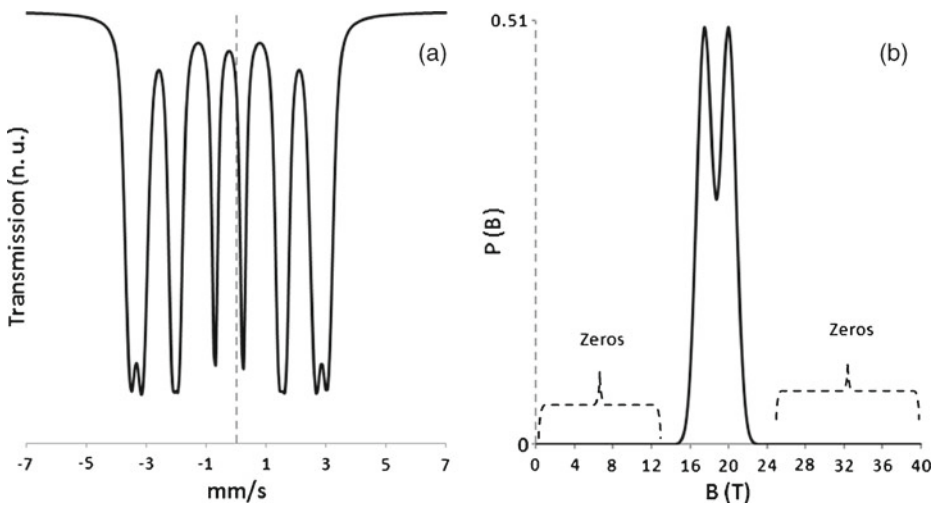


Fig. 1 Hesse and Rübartsch's data [3]. (a) A distributed sextet by (b) two Gaussian lines, centered at 17.5 and 20 T

4 Results

4.1 Hesse and Rübartsch's data

The resolution test data of Hesse and Rübartsch's paper is reanalyzed. Figure 1 shows the corresponding data of example 3. (ii) from reference [3], where a magnetic sextet is distributed by a two Gaussian shaped functions ($P(B)$), centered at the magnetic field values $B = 17.5$ and 20 T and having a standard deviation $\sigma_H = 0.85$ T each, as shown in Fig. 1a and b. A first observation must be made from the two Gaussian distribution function, Fig. 1b: the plotted distribution function $P(B)$ has two regions of zeros as indicated by the keyets.

These zeros appear from 0.0 to 12.5 T and from 25 to 40 T. That is, the integration limits of integral equation (1) should be $c = 12.51$ and $d = 25.1$ T only.

The recovered distribution function $P(B)$ from Fig. 1a when applying the unmodified Window method [3] as suggested in reference [3], using the limits $c = 0$ and $d = 40$ in the integral equation (1), and using 15, 25 and 35 terms of the FSE, is shown in Fig. 2. The resulting distributions have oscillations as those shown in reference (3). The best fit is obtained when using 35 terms of the FSE but still small oscillations are present in the resulting distribution, Fig. 2c'. A little higher oscillations appear if the Lorentzian width of the sextet is fixed to its actual value ($W_L = 0.1926$ mm/s [3]). Such oscillations are removed if the c and d integral limits are, for example 12.5 and 25 T, respectively, or if they are calculated by the program as shown in Fig. 3a', respectively. Two presentations of the resulting distribution can be made, the typical superimposed distribution (Fig. 3a' and the separated one, Fig. 3b'. The squared chi fitting criterion is improved by two orders of magnitude if the integral limits are guessed and the distributions are separated, Fig. 3b'. In the last two cases the line width of the sextet was also evaluated and was recalculated with zero error as shown in the Fig. 3b' case.

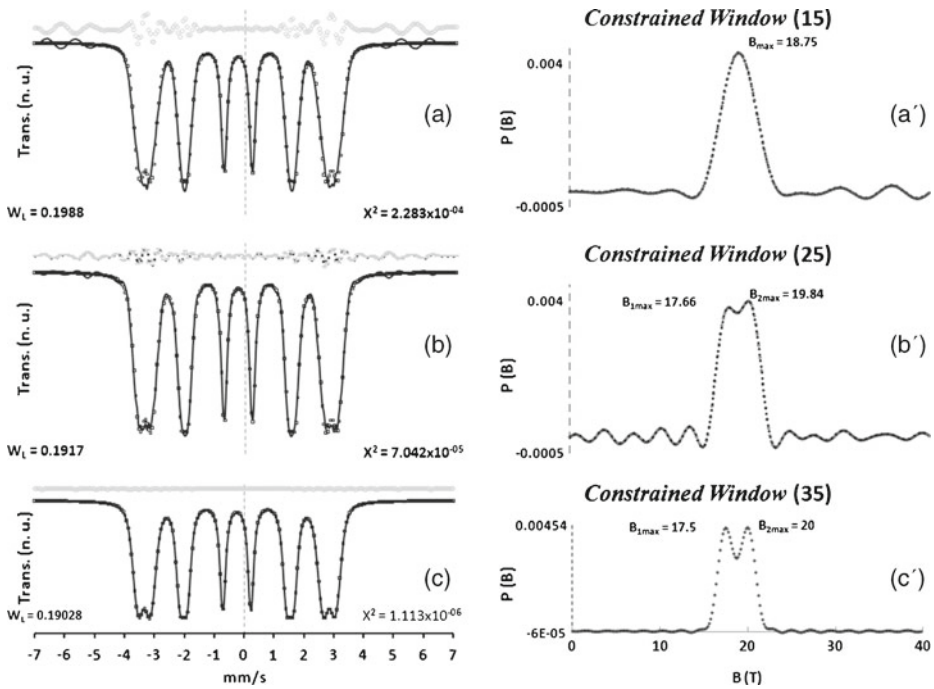


Fig. 2 Hyperfine field distributions by Hesse and Rübartsch [3] using the Window method [2]. On the top of each left figure the un-normalized residuals are plotted. The Lorentzian width W_L was evaluated and was not recovered

The case for which the Gaussian distribution function is replaced by a triangular distribution function is shown in Fig. 3c'. Firstly, note that in this case a single parameter (the number shown in parenthesis in these figures) is only required to define a triangular distribution function. In the present case, the computing program also requires a single parameter to produce both triangles as shown in Fig. 3c'. Thus this triangular distribution speeds up any calculation as compared to those using the Window or other methods. Secondly, it can be noticed from the small residuals that this triangular distribution function is not a bad approximation to the original Gaussian distribution function $P(B)$. The integration limits are also evaluated by the program and in this case the possibilities of oscillations in the fitted spectrum and distribution are also removed.

4.2 S3A magnetic alloy

Following the above strategy, i. e. optimizing the integral limits to prevent any spurious oscillations, the CXMS and transmission spectra of the amorphous soft magnetic alloy S3A, treated at 50C/20' and 430C/20', respectively, are next analyzed. Figure 4 shows two typical hyperfine field distributions (HFD) from the amorphous state of the alloy when using the unmodified [2] and modified Window methods with 6 terms of the FSE (and $\lambda_c = 1.0$) and 12 terms of the FSE (and $\lambda_c = 1.1109$), either evaluating or fixing the intensity ratios of lines two and five (I25) of the magnetic sextet.

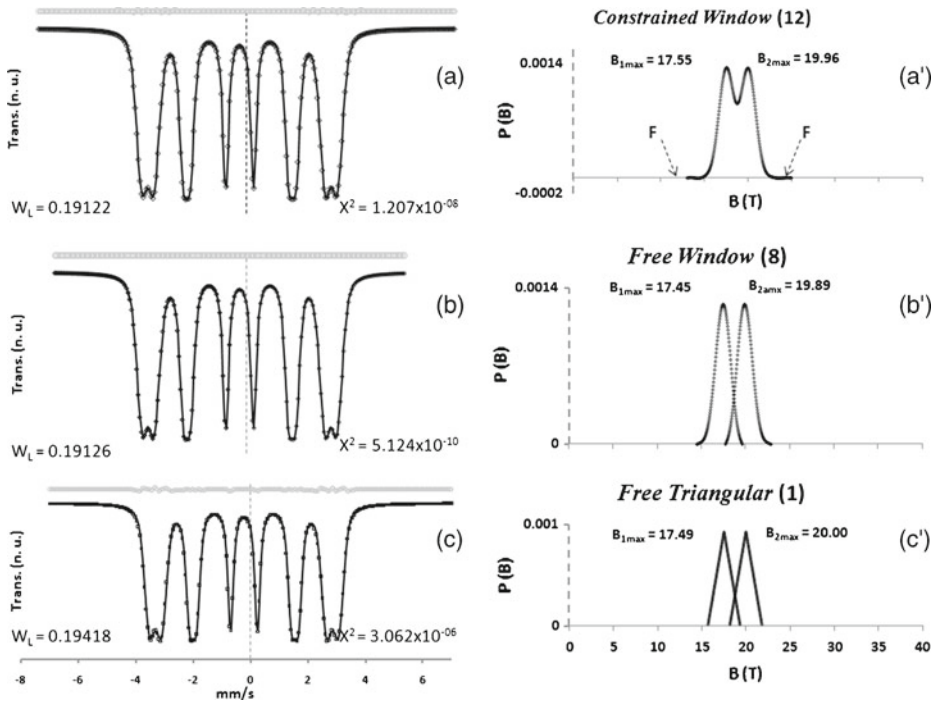


Fig. 3 Oscillations free hyperfine distributions obtained by (a) fixing the c and d integral limits, using 12 terms of the FSE, or (b) guessed using 8 terms of the FS only. The distribution can be obtained as (a) superimposed or (b and c) separated one

A single Gaussian distribution is suggested from Fig. 4a'. A more complex distribution is obtained if 12 terms of the FSE and λ_c is evaluated. The latter distribution will be named as the low resolved hyperfine field distribution (LR-HFD). Whereas Fig. 4a' may suggest a single phase, i. e., the amorphous phase of the alloy, Fig. 4b' might suggest a set of Fe-Cr-Si-B crystalline phases.

From the Mössbauer spectroscopy, and particularly from the LR-HFD, still remains ambiguous if the experimental Mössbauer spectrum of metallic glasses, like the S3A alloy, indeed originates from the amorphous phase (Fig. 4a') or not (Fig. 4b').

A similar LR-HFD was reported by Le Caer and Dubois in 1979 arising from the amorphous alloy $\text{Fe}_{79.5}\text{Si}_{1.5}\text{B}_{19}$ [7]. As a result of this, a great deal of research has been carried out to elucidate the local atomic structure around the iron, boron and phosphorus atoms of these metallic glasses in order to be able to interpret the spectral features of Fig. 4b' suggesting the presence of crystalline material [7–14]. Nowadays is generally believed that the local structure around the boron atoms in metallic glasses possess short-range atomic-order (SRAO) rather than short-range atomic-disorder (SRAD). Research work in this area is still in progress to define such a matter (13, 14). The SRAO perception came after studying ^{10}B NMR spectroscopy in some metallic glasses containing ^{10}B , where sharp NMR peaks arise from different supposedly amorphous Fe-B phases [8, 13].

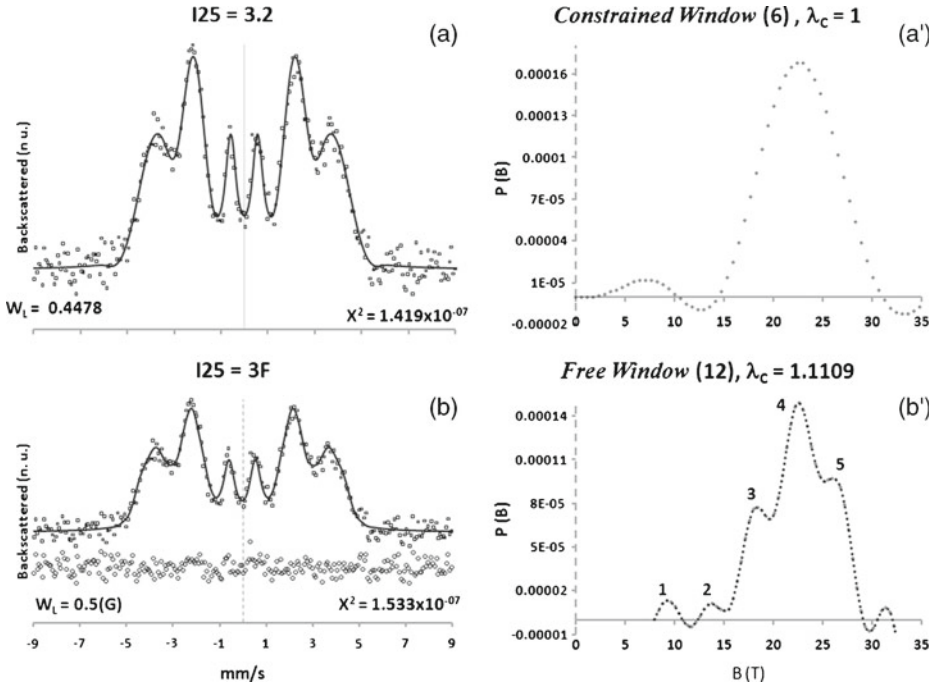


Fig. 4 (a) Fitted CXMS spectrum of the amorphous alloy using the unmodified Window’s method ($\lambda_c = 1$), (a’) an unresolved hyperfine field distribution is obtained when using six terms of the FSE. (b) Fitted CXMS spectrum of the amorphous alloy using the modified Window’s method ($\lambda_c = 1.1109$), (b’) a low resolved hyperfine field distribution is obtained when using 12 terms of the FSE

The question that arose at Le Caer and Dubois’s time (1979) was: Are real the spectral features of the LR-HFD as shown in Fig. 4b’? or they are the product of mathematical artifacts? As far as the author understands, these spectral features appearing in Fig. 4b’ have not been answered quite satisfactorily.

In the present case, the mathematical artifacts (spurious oscillations) can mostly be discharged from Fig. 4b’ due to the fact that the integral limits are optimized and minimal oscillations would be expected. The statistical nature of the present experimental data may also produce additional oscillations. However, this also can be ruled out because the statistical quality of the Mössbauer data of Le Caer and Dubois’s paper [7] is better than in the present case, and in spite of this the obtained distributions and the fitted spectrum are practically the same as those reported by Le Caer and Dubois [7]. In addition to this, no matter if a zero order or a second order regularized algorithm is used. Thus, in order to give, from the Mössbauer point of view, support to the LR-HFD structure of Fig. 4b’, the transmission Mössbauer spectrum (TMS) of the heat treated S3A alloy at 530C/20’ was obtained, which is shown in Fig. 5b.

This TMS was fitted using the trigonometric n th-nomial distribution function $P(x) = (a\cos(\pi x) + b\sin(\pi x))^n$ with $n = 29$. The resulting coefficients of this trigonometric distribution function are evaluated as simple parameters by the program. Take the example case for $n = 2$ where the resulting coefficients are: $a^2, 2ab,$

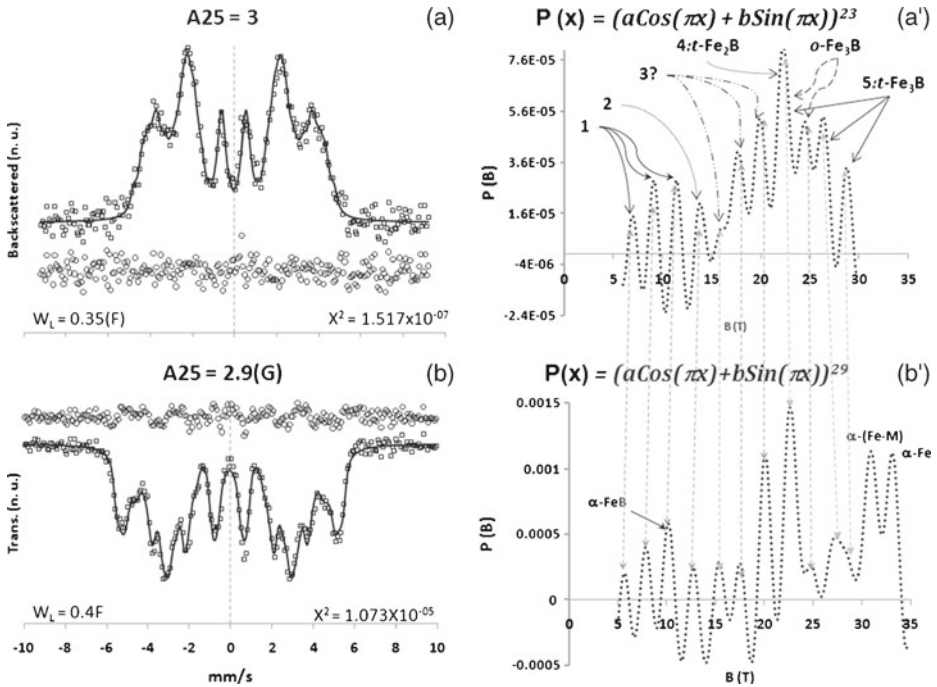


Fig. 5 (a) CXMS Mössbauer spectrum of the amorphous alloy fitted using the trigonometric sum with an exponent $n = 23$; (b) Transmission Mössbauer spectrum of the crystallized alloy fitted using the n th-binomial expansion distribution with $n = 29$

b^2 and the corresponding numerical values are: 1, 2, 1, respectively, with $a = 1$ and $b = 1$. The evaluated coefficients generally differ from the preceding whole numbers.

For comparison purposes, the fitted Mössbauer spectrum and the resulting HFD of the amorphous alloys are also presented in Fig. 5a and a'; in this case a 23th-nomial trigonometric function was used and a high resolved HFD (HR-HFD) is now shown for both these cases, Fig. 5a' and b' having practically the same peak structure for fields lower than 30 T. A small shift is observed between these peaks only. Is it a coincidence such a peak matching? Or is it an evidence of the short-range atomic structure of the amorphous state of the alloy?

Large oscillations with negative values appearing in Figs. 4 and 5b's should not be considered, they were enhanced in order to obtain HR distributions containing the typical information of these alloys [14, 15]. Negative values can be eliminated but LR distributions are obtained which are not useful for the present discussion.

Thus the LR-HFD in Fig. 4b' may be rationalized as follows:

- (i) The small broad peak at 9.25 T, peak 1 shown in the LR-HFD of Fig. 4b', and a first group of three peaks, gathered by curved arrows as shown in the HR-HFD of Fig. 5b', located at 5.47, 7.81 and 10.16 from which an average peak value of 7.81 T is obtained. This average value deviates -15.53% the peak 1 position in Fig. 4b'. If this average value is taken from the HR-HFD of the amorphous material such deviation is less than 1%. Broken lines between peaks of Figs. 4 and 5b' show the corresponding shifts.

- (ii) The next smaller peak at 13.83 T in Fig. 4b' (peak 2) practically matches its position with the peak at 13.8 T from the HR-HFD in Fig. 5a'. From Fig. 5b', i. e. from the crystallized material this peak is at 12.73 T which deviates a -7.7% .
- (iii) Peak 3 from the LR-HFD in Fig. 4b' is located at 18.4 T. The next gathered three peaks from the HR-HFD signalized by a (3?) in Fig. 5a' are located at 15.97, 17.58 and 19.65 T, making them an average value of 17.7 T, which deviates a -3.6% from peak 3 in Fig. 4b'. The corresponding average value from these peaks in Fig. 5b' is 17.58 %, i. e., -4.47%
- (iv) The highest peak of the LR-HFD in Fig. 4b' (peak number 4) is at 22.58 T. The corresponding highest peak of the HR-HFD in Fig. 5a' signalized by (4, $t\text{-Fe}_2\text{B}$) is located at 21.95 T, which deviates -2.7% from peak 4 in Fig. 4b. The central peak position from Fig. 5b' is 22.58 T, i. e., the same as in the amorphous state. This peak actually arises from a superposition of several ones as next explained and supported by references [16, 17].
- (v) The next peak to follow from the LR-HFD in Fig. 4b' is peak number 5 which is located at 25.92 T. The gathered three peaks from the HR-HFD identified by 5: $\alpha\text{-Fe}_3\text{B}$ in Fig. 5a' are located at 2.95, 26.09 and 28.38 T, making an average value of 25.47 T, which deviates -1.71% from peak 5 in Fig. 4b'. The corresponding average value of from Fig. 5b' is 25.85 T, with less than 1 % deviation.
- (vi) Peak number 6 in Fig. 4b' was not matched with none of Fig. 5a' and b'.

It can be inferred from the above analysis that the LR-HFD distribution of this amorphous material arises from a large superposition of Mössbauer patterns arising from different iron sites.

The peak structure shown in Fig. 5b' is very well known in the literature [14, 15] in such a way that every peak has practically been identified for some particular Fe-phases as indicated in Fig. 5a' and b'. Those peaks identified by (3?) in Fig. 5b' may have different origin depending on the alloy under study [14, 15]. The main point to enhance here is that every peak belongs to a magnetic material in its crystallized form (16, 17).

Based on this analysis, the LR-HFD peaks arising from the Mössbauer spectrum of the amorphous alloy may be interpreted as a result of average values that arise from the corresponding hyperfine magnetic fields of the involved crystallized Fe-B phases for each soft magnetic alloy (8, 13, 14, 15). Thus the present amorphous alloy would consist of a mixture of Fe-B phases having SRAO [7–17], and it can be concluded that one is able to infer unambiguously from the LR- and HR-HFD's of the Mössbauer spectra of the amorphous alloy the presence of SRAO.

5 Conclusions

The Hesse and Rübartsch data were reanalyzed using the unmodified Window method [3] and the Levenberg-Marquardt algorithm. It was shown from this analysis that, the oscillations shown in the Hesse and Rübartsch paper [4] arise from rounding errors mainly and they can be removed completely by taking care of the integration limits (c and d) of integral equation (1). In addition to this the triangular function was introduced in this work as an approximation to the Gaussian distribution function

giving satisfactory results. On the other hand, experimental Mössbauer spectra of the amorphous and crystallized magnetic S3A alloy were analyzed using the new no implicit distribution function $P(x) = (a\cos(\pi x) + b\sin(\pi x))^n$. The main result of this analysis indicates that the low and high resolved structures appearing in the HFD of the amorphous material may be real. The LR-HFD of the amorphous alloy can be interpreted as arising from average values due to the different Fe-B phases as detected in the high resolved HFD of the crystallized alloy. Similarly, from the comparison between the HR-HFD of the amorphous and crystallized alloy a direct comparison can be made. Practically the same number of peaks appears in both these highly resolved distributions, suggesting therefore the presence of SRAO in the amorphous S3A alloy. The shift between these peaks may be associated to the particular properties of the SRAO and LRAO solids. That is, the CXMS spectrum comes from the surface and the TMS spectrum from the bulk. Such a shift may be associated with different hyperfine parameters between the Mössbauer spectra of the surface and bulk material.

Acknowledgement We thank to Dr. R. Hasegawa from Metglass Inc. Co. USA for his donation of a long ribbon of the 2605 S3A amorphous alloy.

References

1. Varret, F., Gerard, A., Imbert, P.: *Phys. Stat. Solidi B* **43**, 423 (1971)
2. Window, B.: *J. Phys. E: Sci. Instrum.* **4**, 401 (1971)
3. Hesse, J., Rübartsch, A.: *J. Phys. E: Sci. Instrum.* **7**, 526 (1974)
4. Gonser, U., Ghafari, M., Wagner, H.G.: *J. Magn. Magn. Mater.* **8**, 175 (1978)
5. Vincze, I., Babic, E.: *Solid State Commun.* **25**, 689 (1978)
6. Vincze, I., Babic, E.: *Solid State Commun.* **27**, 1425 (1978)
7. Le Caer, G., Dubois, J.M.: *J. Phys. E: Sci. Instrum.* **12**, 1083 (1979)
8. Ford, J.C., Budnick, J.I., Hines, W.A., Hasegawa, R.: *J. Appl. Phys.* **55**, 2268 (1984)
9. Dubois, J.M., Le Caer, G.: *J. Physique Colloque* **43**, C9(12), C9–67 (1982)
10. Kopcewicz, M., Wagner, H.G., Gonser, U.: *J. Physique Colloque* **46**, C8(12), C8–151 (1985)
11. Eibschüts, M., Lines, M.E., Chen, H.S., Matsumoto, T.: *J. Phys. F: Met. Phys.* **14**, 505 (1984)
12. Ideczak, R., Konieczny, R., Chojean, J.: *Hyperfine Interact* **208**, 1 (2012). doi:10.1007/s10751-011-0458-6
13. Pokatilov, V.S.: *Phys. Solid State* **49**(12), 2217 (2007)
14. Pokatilov, V.S., Dimitrieva, T.G., Pokatilov, V.V., D'yakonova, N.B.: *Phys. Solid State* **54**(9), 1790 (2012)
15. Barinov, V.A., Tsurin, V.A., Voronin, V.I., Surikov, V.T.: *Phys. Met. Metallogr.* **108**(1), 50 (2009)
16. Frank, H., Rsenberg, M.: *J. Magn. Magn. Mater.* **7**, 168 (1978)
17. Sánchez, F.H., Zhang, Y.D., Budnick J.I., Hasegawa R.: *J. Appl. Phys.* **66**(4), 1671 (1989)